











## ARTICLE

# The adiponectin-derived peptide ALY688 protects against the development of metabolic dysfunction-associated steatohepatitis

Zhe Huang<sup>1,2,3</sup>  | Hye Kyoung Sung<sup>4</sup>  | Xingqun Yan<sup>1,2</sup>  | Shiyu He<sup>1,2</sup>  |  
Leigang Jin<sup>1,2</sup>  | Qin Wang<sup>1,2</sup>  | Xuerui Wu<sup>1,2</sup>  | Henry H. Hsu<sup>5</sup>  |  
Angelica Pignalosa<sup>5</sup>  | Kathryn Crawford<sup>5</sup>  | Gary Sweeney<sup>4</sup>  | Aimin Xu<sup>1,2,6</sup> 

<sup>1</sup>The State Key Laboratory of Pharmaceutical Biotechnology, The University of Hong Kong, Hong Kong, China

<sup>2</sup>Department of Medicine, The University of Hong Kong, Hong Kong, China

<sup>3</sup>Department of Genetics and Developmental Science, School of Life Sciences and Biotechnology, Shanghai Jiao Tong University, Shanghai, China

<sup>4</sup>Department of Biology, York University, Toronto, Ontario, Canada

<sup>5</sup>Allysta Pharmaceuticals, Bellevue, Washington, USA

<sup>6</sup>Department of Pharmacology and Pharmacy, The University of Hong Kong, Hong Kong, China

## Correspondence

Aimin Xu, The State Key Laboratory of Pharmaceutical Biotechnology, Department of Medicine, The University of Hong Kong, Laboratory Block, 21 Sassoon Road, Pokfulam, Hong Kong, China.  
Email: [amxu@hku.hk](mailto:amxu@hku.hk)

## Abstract

Metabolic dysfunction-associated steatohepatitis (MASH) is the severe form of non-alcoholic fatty liver disease which has a high potential to progress to cirrhosis and hepatocellular carcinoma, yet adequate effective therapies are lacking. Hypoadiponectinemia is causally involved in the pathogenesis of MASH. This study investigated the pharmacological effects of adiponectin replacement therapy with the adiponectin-derived peptide ALY688 (ALY688-SR) in a mouse model of MASH. Human induced pluripotent stem (iPS) cell-derived hepatocytes were used to test cytotoxicity and signaling of unmodified ALY688 in vitro. High-fat diet with low methionine and no added choline (CDAHf) was used to induce MASH and test the effects of ALY688-SR in vivo. Histological MASH activity score (NAS) and fibrosis score were determined to assess the effect of ALY688-SR. Transcriptional characterization of mice through RNA sequencing was performed to indicate potential molecular mechanisms involved. In cultured hepatocytes, ALY688 efficiently induced adiponectin-like signaling, including the AMP-activated protein kinase and p38 mitogen-activated protein kinase pathways, and did not elicit cytotoxicity. Administration of ALY688-SR in mice did not influence body weight but significantly ameliorated CDAHf-induced hepatic steatosis, inflammation, and fibrosis, therefore effectively preventing the development and progression of MASH. Mechanistically, ALY688-SR treatment markedly induced hepatic expression of genes involved in fatty acid oxidation, whereas it significantly suppressed the expression of pro-inflammatory and pro-fibrotic genes as demonstrated by transcriptomic analysis. ALY688-SR may represent an effective approach in MASH treatment. Its mode of action involves inhibition of hepatic steatosis, inflammation, and fibrosis, possibly via canonical adiponectin-mediated signaling.

This is an open access article under the terms of the [Creative Commons Attribution-NonCommercial-NoDerivs](https://creativecommons.org/licenses/by-nc-nd/4.0/) License, which permits use and distribution in any medium, provided the original work is properly cited, the use is non-commercial and no modifications or adaptations are made.

© 2024 The Authors. *Clinical and Translational Science* published by Wiley Periodicals LLC on behalf of American Society for Clinical Pharmacology and Therapeutics.

### Study Highlights

#### WHAT IS THE CURRENT KNOWLEDGE ON THE TOPIC?

Hypoadiponectinemia is causally involved in the pathogenesis of metabolic dysfunction-associated steatohepatitis (MASH), that may ultimately lead to cirrhosis and hepatocellular carcinoma. Accordingly, strategies to boost adiponectin action are proposed to be beneficial in treating MASH. However, multiple technical challenges have hindered therapeutic development of native adiponectin protein or small molecule adiponectin receptor agonists.

#### WHAT QUESTION DID THIS STUDY ADDRESS?

This study investigated the effects of ALY688, a peptide agonist of adiponectin receptors, in a preclinical mouse model of MASH and examined the underlying mechanisms of action.

#### WHAT DOES THIS STUDY ADD TO OUR KNOWLEDGE?

ALY688 induced adiponectin-like signaling without cytotoxic effects in hepatocytes. Notably, ALY688 effectively alleviated the development of MASH and its progression to hepatic fibrosis in a mouse model of MASH. These effects were achieved via induction of hepatic fatty acid oxidation and inhibition of both hepatic inflammation and fibrogenesis.

#### HOW MIGHT THIS CHANGE CLINICAL PHARMACOLOGY OR TRANSLATIONAL SCIENCE?

The protective effects of ALY688 against MASH support the potential therapeutic application of this peptide in the clinic for treatment of MASH in the future.

## INTRODUCTION

Metabolic dysfunction-associated steatotic liver disease (MASLD) is strongly associated with obesity and its related metabolic complications.<sup>1</sup> It affects more than a quarter of the population worldwide with a rapidly rising prevalence in parallel with the global epidemic of obesity. MASLD comprises a spectrum of liver diseases ranging from simple steatosis to metabolic dysfunction-associated steatohepatitis (MASH).<sup>2</sup> While simple steatosis is characterized by excessive lipid accumulation in the liver, which is generally a benign condition, MASH is the advanced stage of MASLD characterized by not only lipid accumulation, but also hepatic inflammation and necrosis of hepatocytes.<sup>2</sup> MASH is generally considered as an irreversible disease as it can also prompt collagen synthesis and deposition, leading to end-stage liver diseases, including cirrhosis and hepatocellular carcinoma (HCC).<sup>2</sup> Indeed, the prevalence of MASLD-associated HCC has strikingly increased over the last few decades due to the global epidemic of metabolic disorders. MASH and metabolic etiology of HCC has replaced viral hepatitis as the leading cause of HCC nowadays.<sup>3</sup> Furthermore, different etiology of HCC may produce different responsiveness to systemic therapies. In this regard, non-viral etiology of HCC has been found

to be associated with a better prognosis in patients treated with lenvatinib, a multi-tyrosine kinase inhibitor, than viral etiology.<sup>4</sup> Although the pathogenesis of MASH is not fully elucidated, it is generally agreed that abnormal lipid accumulation in the liver, lipotoxicity, hepatic inflammation, and gut dysbiosis are all contributing factors to MASH development.<sup>5</sup> However, currently there are no established therapeutics effectively targeting MASH, probably due to the multifactorial nature of this disease.

Adiponectin is one of the most abundant adipokines secreted by adipocytes.<sup>6</sup> Adiponectin possesses pleiotropic effects on the regulation of insulin sensitivity, lipid catabolism, and inflammation in various tissues via interacting with its receptors, adipoR1 and adipoR2.<sup>7</sup> Circulating levels of adiponectin are decreased in both rodents and human patients with obesity and are inversely correlated with insulin resistance.<sup>8</sup> Hypoadiponectinemia has also been associated with MASH. Patients with biopsy-proven MASH had a significantly lower serum level of adiponectin than those with simple steatosis independent of insulin resistance.<sup>9</sup> Circulating adiponectin levels are negatively associated with hepatic necroinflammation.<sup>9</sup> Adiponectin circulates mainly in high molecular weight (HMW) oligomeric and medium-molecular weight hexameric forms,

and to a lesser extent, low molecular weight trimeric forms. Although total adiponectin was measured in most studies and the HMW form of adiponectin is generally agreed to be more closely associated with insulin resistance and obesity,<sup>10</sup> there has been no significant difference in the distribution of adiponectin isoforms between MASH patients and healthy individuals.<sup>11</sup> Rather, animal studies suggest that overall hypoadiponectinemia is causally involved in MASH. For example, adiponectin knockout mice were more prone to develop cirrhosis and even hepatic tumors than wild-type mice when fed with a choline-deficient L-amino acid-defined diet, which is used to induce MASH.<sup>12</sup> Adiponectin deficiency also accelerated MASH development with increased oxidative stress and Kupffer cell polarization in mice fed with a methionine choline-deficient (MCD) diet.<sup>13</sup> Transgenic mice expressing nuclear sterol regulatory element-binding protein 1c (nSREBP-1c) in adipose tissue developed spontaneous MASH and hypoadiponectinemia as they aged; whereas the MASH liver phenotype was decelerated in nSREBP-1/adiponectin double transgenic mice, that paralleled with lower ER stress.<sup>14</sup> Moreover, pharmacological administration of recombinant full-length mouse adiponectin alleviated MASLD in *ob/ob* mice potentially by induction of fatty acid oxidation and suppression of inflammation in the liver.<sup>15</sup>

Despite the hepatoprotective effects of adiponectin as shown in the aforementioned studies, development of adiponectin replacement therapy for treatment of MASH based on recombinant proteins has been hindered by several challenges. First, the extreme insolubility of the C-terminal globular domain and larger peptide fragments limits the generation of the full-length protein.<sup>16</sup> Second, the heterogenous nature of adiponectin isoforms produces non-reproducible results between *in vitro* and *in vivo* experiments.<sup>17</sup> In addition, different isoforms have different biodistribution in tissues, especially where the HMW form is considered most active, yet less likely to penetrate tissues due to its large size. Small molecule-based adiponectin mimetics have emerged in the last decade to fill the gap. Among them, an adiponectin-derived peptide named ALY688-acetate (ALY688), also referred to as ADP355, has been developed.<sup>18</sup> It is a 10-amino acid (10-mer) short peptide covering the active site of the adiponectin globular domain with a molecular weight of ~1100 Da so that it can easily penetrate into tissues. It has been shown to activate both adipoR1 and adipoR2, eliciting adiponectin-like signaling in various cell types.<sup>18</sup> It has been shown to exert liver protective effects against thioacetamide (TAA)-induced liver injury and carbon tetrachloride (CCl<sub>4</sub>)-induced liver fibrosis in mice.<sup>19</sup> However, the effects of

ALY688 on MASH has not been investigated. Although recently a 6-mer globular adiponectin-based adipoR agonist JT003 has been suggested to recover MASH via the endoplasmic reticulum–mitochondria axis, this conclusion was made mainly based on a mouse model with 16-week high-fat diet, which only produces steatosis, but not MASH as evidenced by the histological data in the same study.<sup>20</sup> In addition, JT003 is relatively short-acting with a half-life of approximately 45 min.<sup>20</sup>

In this study, we established experimental MASH models using high-fat diet with low methionine and no added choline (CDAHf)<sup>21</sup> and high-fat diet fed to mice with streptozotocin (STZ)-induced insulin insufficiency<sup>22</sup> to evaluate the effects of ALY688. We found that administration of ALY688, and especially ALY688-SR, protected mice against the development of MASH and fibrosis by increasing lipid catabolism and decreasing inflammation and fibrogenesis in the liver.

## METHODS

### Animals

For pharmacokinetic assay, male Sprague–Dawley (SD) rats were purchased from Charles River Laboratories and adapted to the animal facility with *ad libitum* access to water and a certified laboratory diet. Two rats were housed per cage. All rats were maintained under controlled conditions of temperature (22–24°C), humidity, and lighting (12-h artificial light and dark cycles). All animals used in this study were housed and cared for in accordance with the Guide for the Care and Use of Laboratory Animals (ILAR Publication, 2011, National Academy Press).

For the streptozotocin and high-fat diet (STAM) model, C57BL/6 mice (14-day pregnant female) were obtained from Japan SLC (Japan). The animals were maintained in a specific pathogen-free facility under controlled conditions of temperature (23±2°C), humidity (45±10%), lighting (12-h artificial light and dark cycles; light from 8:00 to 20:00), and air exchange. Gamma-irradiated solid high-fat diet was provided *ad libitum*, from the top of the cage. Drinking water was provided *ad libitum* by water bottle that was replaced once a week. All animals used in the study were housed and cared for in accordance with the Japanese Pharmacological Society Guidelines for Animal Use.

For the CDAHf model, C57BL/6N male mice at 6 weeks of age were purchased from the Centre for Comparative Medicine Research of the University of Hong Kong (CCMR, HKU) and adapted to the animal facility with

ad libitum access to water and standard chow (STC) diet (LabDiet 5053, Saint Louis, MO, USA) until they reached 8 weeks of age. All animals were maintained under controlled conditions of temperature (22–24°C), humidity, and lighting (12-h artificial light and dark cycles). All animal experiments were approved by the Committee on the Use of Live Animals in Teaching and Research at the University of Hong Kong.

## Pharmacokinetic study

Male adult SD rats were administered a single subcutaneous (s.c.) injection of ALY688 (unmodified form) at 10 mg/kg and ALY688-SR (sustained release form) at 20 mg/kg. Blood samples were collected at 30 min and 1, 2, 4, 8, 24, 48, 72, 96, 144, and 192 h following the injection and immediately centrifuged at 4°C at 2500×g for 10 min to obtain plasma samples. Plasma concentrations of the peptides were measured by liquid chromatography/tandem mass spectrometry (LC-MS/MS) (ThermoFisher Scientific, Waltham, MA, USA). Pharmacokinetic parameters ALY688 and ALY688-SR were calculated using Phoenix® WinNonlin® version 8.0 (Certara, Clayton, MO, USA). Concentration values less than the lower limit of quantitation (LLOQ) were set to zero for the analysis.

## General experimental procedures for mouse studies

For the STAM model, male C57BL/6N mice at 2 days after birth received a single s.c. injection of 200 µg STZ (Sigma-Aldrich, St. Louis, MO, USA) solution; these mice were fed with high-fat diet (HFD, 57 kcal% fat, Cat# HFD32, CLEA Japan, Tokyo, Japan) from 4 to 9 weeks of age to induce MASH.<sup>22</sup> From 6 to 9 weeks of age, the mice were administered with vehicle or two doses of ALY688 (low: 0.5 mg/kg/day, high: 5 mg/kg/day) via daily s.c. or continuous s.c. infusion via osmotic pumps (OP; Cat# 2004, Alzet, Cupertino, CA, USA) at an infusion rate of 0.25 µL/h. Mice were randomized into two cages of three for each of the five treatment groups ( $N=6$ /treatment group).

For the CDAHf model,<sup>21</sup> male C57BL/6N mice at 8 weeks of age were fed with choline-deficient with low methionine high-fat diet (CDAHFD, 60 kcal% fat, Cat# CDAHf60, Dyets, Bethlehem, PA, USA) for 12 weeks to induce MASH. Three weeks after CDAHFD feeding, the mice were treated with ALY688-SR (low: 3 mg/kg/day, high: 15 mg/kg/day) or vehicle by daily s.c. injection for

9 weeks. Mice treated with obeticholic acid (OCA, 30 mg/kg) by daily oral gavage were used as the positive control group, STC-fed mice treated with vehicle were considered as the negative control group. Mice were randomized into two cages of five for each of the five treatment groups ( $N=10$ /treatment group).

## Measurement of body composition

Lean, fat tissue, and free fluid in living mice were measured using the Bruker Minispec LF90 II NMR body composition analyzer.

## Measurement of serum and hepatic ALY688-SR

At the end of the CDAHf study, the animals were sacrificed, and terminal blood samples by cardiac puncture and liver tissues were collected after 1 h of the ALY688-SR injection and shipped to AIT BioScience (Indianapolis, IN, USA) for bioanalytical quantification. Briefly, tissue samples were transferred to 7 mL Precellys tubes and weighed. To effect liver tissue homogenization, 2–3 zirconium oxide 2.8 mm beads and 6–12 zirconium oxide 1.4 mm beads were added to each sample tube. The tissue was then diluted 10× with blank mouse plasma. Following addition of the plasma to each tissue sample, samples were homogenized on the Precellys at 6500 rpm for 3×30 s. A sample volume of 25 µL was aliquoted into a 1.2 mL 96-well plate and mixed with 12 µL internal standard solution (10 ng/mL ALY688-D7 in water: acetonitrile, 50:50). The peptide concentrations in the serum and liver were measured by LC-MS/MS (ThermoFisher Scientific). Raw data from the mass spectrometer were acquired and processed with the Thermo Scientific Watson Laboratory Information Management System. Peak area ratios from the calibration standard responses were regressed using a  $(1/\text{concentration}^2)$  linear fit for ALY688. The regression model was chosen for analysis based on the behavior of the analyte across the concentration range used.

## Measurement of serum adiponectin

At the end of the CDAHf study, terminal blood samples were collected, and serum level of adiponectin was determined using the mouse adiponectin enzyme-linked immunosorbent assay (ELISA) kit (Cat# 32010, ImmunoDiagnostics Limited, Hong Kong).

## Evaluation of liver injury markers

For the STAM model, plasma alanine transaminase (ALT) and aspartate transaminase (AST) levels were measured by FUJI DRI-CHEM 7000 (Fujifilm, Japan). For the CDAHf model, plasma ALT and AST were measured by commercial assays (Cat# 2930 and #2920, Stanbio Laboratory, Boerne, TX, USA) according to the manufacturer's instructions.

## Hepatic triglyceride content

Total liver lipids were extracted as previously described.<sup>23</sup> Hepatic triglyceride (TG) content was quantified using a commercial kit (Cat# BD386, Stanbio Laboratory) according to the manufacturer's instructions.

## Histological analysis and NAS evaluation

Paraformaldehyde-fixed (4%) liver samples were paraffin-embedded, sliced into 10  $\mu$ m sections, and stained with hematoxylin and eosin (H&E) for the evaluation of severity of hepatocellular steatosis, inflammation, ballooning, and fibrosis according to the MASH Clinical Research Network (CRN) Scoring System.<sup>24,25</sup>

## Association of collagen deposition in liver

The paraffin-embedded liver sections were stained with Masson's trichrome (Cat# ab150686, abcam, Cambridge, UK) and Picro Sirius Red (Cat# ab150681, abcam) for collagen deposition according to the manufacturer's instructions. Quantitative morphometric measurements were processed as previously described.<sup>26</sup>

## Immunoblotting

Proteins were extracted from liver tissues in the presence of the protease inhibitors cocktail, resolved by sodium dodecyl-sulfate polyacrylamide gel electrophoresis (SDS-PAGE) and transferred to polyvinylidene fluoride (PVDF) membranes. The membranes were probed with the antibody against  $\alpha$ -SMA (Cat# ab5694, abcam) and GAPDH (Cat# 2118, Cell Signaling Technology, Danvers, MA, USA) followed by incubation with anti-rabbit antibody conjugated with horseradish peroxidase (Cat# #7074, Cell Signaling Technology). Proteins in the membrane were finally visualized with enhanced chemiluminescence reagents exposed by a ChemiDoc MP Imaging System (BioRad, Hercules, CA, USA). The intensity of protein bands

was quantified by using the ImageJ software (National Institutes of Health).

## Measurement of hepatic hydroxyproline

Hepatic hydroxyproline levels were measured using a commercial kit (Cat# ab222941, abcam) according to the manufacturer's instructions.

## RNA extraction and RT-qPCR

Total RNA was isolated from liver tissues using RNAiso plus according to the manufacturer's instructions (Cat# 9108, Takara, Shiga, Japan) and reverse-transcribed into complementary DNA using RT kits (Cat# RR037B, Takara, Japan). Real-time quantitative polymerase chain reaction (RT-qPCR) was performed using SYBR Green Master Mix (Cat# RR820L, Takara) for the analysis of hepatic expression of fatty acid oxidation-related genes (*Acot1*, *Acox1*, and *Cyp4a12*), pro-inflammatory genes (*Tnf- $\alpha$* , *IL-1 $\beta$* , and *Mcp-1*), and fibrotic markers (*Tgf- $\beta$* , *Timp1*, and *Col1A1*). The relative gene expression was normalized against the housekeeping gene 18S.

## qPCR primers

Mouse *Acot1*:

Fw: ATACCCCCTGTGACTATCCTGA, Rv: CAAACAC TCACTACCCAACCTGT

Mouse *Acox1*:

Fw: TAACTTCCTCACTCGAAGCCA, Rv: AGTTCCAT GACCCATCTCTGTC

Mouse *Cyp4a12*:

Fw: CCTCTAATGGCTGCAAGGCTA, Rv: CCAGGTG ATAGAAGTCCCATCT

Mouse *Tnf- $\alpha$* :

Fw: ACGGCATGGATCTCAAAGAC, Rv: AGATAGCA AATCGGCTGACG

Mouse *IL-1 $\beta$* :

Fw: ACGGCATGGATCTCAAAGAC, Rv: AGATAGCA AATCGGCTGACG

Mouse *Mcp-1*:

Fw: TTAAAAACCTGGATCGGAACCAA, Rv: GCATT AGCTTCAGATTTACGGGT

Mouse *Col1a1*:

Fw: CCTCAGGGTATTGCTGGACAAC, Rv: CAGAAG GACCTTGTTTGCCAGG

Mouse *Timp1*:

Fw: GCAACTCGGACCTGGTCATAA, Rv: CGGCCCG TGATGAGAACT

Mouse Tgf $\beta$ :

Fw: CTCCCCTGGCTTCTAGTGC, Rv: GCCTTAGTTT  
GGACAGGATCTG

Mouse 18S:

Fw: GGACCAGAGCGAAAGCATTGCG, Rv: TCAAT  
CTCGGGTGGCTGAACGC

## Transcriptomic analysis

At the end of the CDAHf study, total RNA was isolated from liver samples of vehicle and high dose of ALY688-SR-treated mice fed with CDAHf using RNAiso plus. The quality and integrity of purified RNA were examined with the NanoPhotometer<sup>®</sup> spectrophotometer (Implen, Westlake Village, CA, USA) and RNA Nano 6000 assay kit of the Bioanalyzer 2100 system (Agilent Technologies, Santa Clara, CA, USA). Sequencing libraries were generated using NEBNext<sup>®</sup> Ultra<sup>™</sup> RNA Library Prep kit for Illumina<sup>®</sup> (New England Biolabs, Ipswich, MA, USA) following the manufacturer's protocol. Paired-end sequencing was performed at Novogene, Guangzhou, China, with a sequencing depth of ~40 million reads per sample. RNA sequencing raw data were analyzed using a combination of programs including STAR (v2.5) and HTseq (v0.6.1) for mapping reads to a reference mouse genome, quantification, and finally differential expression analysis using the DESeq2 (v2\_1.6.3)/EdgeR (v3.16.5).

## Cell culture, cytotoxicity assay, and signaling assay

For the cytotoxicity assay, human induced pluripotent stem (iPS) cell-derived hepatocytes were incubated with 0.5, 1, 100, 500, 1000, 1500, and 2000 nM of ALY688, 1  $\mu$ g/mL of globular adiponectin (gAd), or 500  $\mu$ M of hydrogen peroxide (H<sub>2</sub>O<sub>2</sub>) for 4 and 24 h. Cytotoxicity was assessed and quantified using MTT formazan (Cat. No. 57360-69-7, Sigma Aldrich) and lactate dehydrogenase (LDH) release according to the manufacturer's instructions (Cat. No. 786-210, G-Biosciences, St. Louis, MO, USA).

For evaluation of adiponectin-like signaling, human induced pluripotent stem (iPS) cell-derived hepatocytes were treated with 0.01, 0.1, 0.5, 1, 100, 200, 300, 500, 700, and 1000 nM of ALY688, 1  $\mu$ g/mL of gAd, 10  $\mu$ g/mL full-length adiponectin (fAd), 1  $\mu$ g of anisomycin (for pP38MAPK assay), or 10  $\mu$ M of AdipoRON (for pAMPK assay) for 30 min. The level of phosphorylation of AMP-activated protein kinase (AMPK) in human induced pluripotent stem (iPS) cell-derived hepatocytes was determined using an ELISA kit (EnzyFluo<sup>™</sup> AMPK Phosphorylation Assay Kit, BioAssay systems, EAMPK-100) to measure AMPK- $\alpha$

phosphorylation at Thr172, following the manufacturer's instructions. The level of phosphorylation of p38 mitogen-activated protein kinase (MAPK) T180/Y182 in human induced pluripotent stem (iPS) cell-derived hepatocytes was determined using an ELISA kit (p38 MAPK alpha (Thr180/Tyr182) In-Cell ELISA Kit, abcam AB126425) to measure p38 MAPK phosphorylation at Thr180/Tyr182, following the manufacturer's instructions.

## Data and statistical analysis

All the data analyses were performed with GraphPad Prism 8.0 (GraphPad, San Diego, CA, USA). Data were presented as mean  $\pm$  standard error of mean (SEM). All experiments were repeated at least three times with representative data shown. Sample sizes of animal studies were chosen based on our previous experience with similar experiments.<sup>27</sup> Statistical significance was determined by unpaired two-sided Student's *t*-test. In all statistical analysis, a *p*-value of <0.05 was considered as a statistically significant difference.

## Materials

ALY688 (Lot# ALL.0918.BR.01 and GM-ALL-03-49) and ALY688-SR (Lot# ALL.1278.BR.01) were provided by Allysta Pharmaceuticals (Bellevue, WA, USA) for study with the STAM model and CDAHf models, respectively. To prepare dosing solutions, ALY688 was diluted in vehicle (0.9% sterile saline). OCA was purchased from Shanghai Hope-Chem Co., Ltd. and freshly dissolved in 0.5% carboxymethylcellulose sodium salt (CMC, Cat# C5678, Sigma-Aldrich) and 0.01% Tween-80 and for oral administration.

## RESULTS

### ALY688 shows no cytotoxicity but induces adiponectin-like signaling in human hepatocytes

To test the cytotoxicity of ALY688 peptides in hepatocytes, human induced pluripotent stem (iPS) cell-derived hepatocytes were incubated with ALY688 at concentrations ranging from 0.5 to 2000 nM. No toxicity was observed with addition of ALY688 even at the highest concentration tested or with the globular adiponectin as the control protein in either 3-(4,5-dimethyltriazol-2-yl)-2,5-diphenyl-2H-tetrazolium bromide (MTT) or lactate dehydrogenase (LDH) assays (Figure S1A,B).

As several signaling pathways involving the energy-sensing AMP-activated protein kinase (AMPK) and p38 mitogen-activated protein kinase (MAPK) are known to mediate the metabolic effects of adiponectin,<sup>28</sup> the effects of ALY688 on phosphorylation of AMPK and p38 MAPK in hepatocytes was assessed using ELISA. ALY688 was demonstrated to induce adiponectin-like signaling in hepatocytes as evident by the phosphorylation of both AMPK and p38 MAPK. Phosphorylation of p38 MAPK at T180/Y182 was significantly enhanced by addition of ALY688 at 100–1000 nM, whereas the statistically significant changes in phosphorylation of AMPK at T172 were observed by treating with ALY688 at 700–1000 nM (Figure S1C,D). Notably, the magnitude of maximum response elicited by ALY688 was similar to that induced by globular adiponectin at 1 µg/mL.

### ALY688 slows the development of MASH in the STAM mouse model

We next examined the efficacy of ALY688 treatment in the progression of MASH in a mouse STAM model. In this model, mice were given a mild dose of STZ via s.c. injection 2 days postnatal to partially destroy beta cells and impair insulin secretion, followed by feeding with an HFD from 4 to 9 weeks of age to induce MASH.<sup>22</sup> The mice were administered with 0.5 or 5 mg/kg of ALY688 or vehicle solution by daily s.c. injection or continuous subcutaneous infusion via osmotic pumps at 2 weeks after initiation of HFD feeding when steatosis is established (Figure 1a). Administration of ALY688 did not induce change in body weight during the treatment period (Figure 1b). The apparent divergence in body weight between the osmotic pump and the injected groups, between weeks 6 and 7, was likely due to the weight of implanted osmotic pump. Treatment with ALY688 by daily s.c. injection did not affect serum ALT and AST levels, markers of liver injury. Although mice with continuous infusion of low-dose ALY688 showed similar levels of serum ALT and AST with vehicle-treated mice, mice with infusion of high-dose ALY688 exhibited slightly lower levels of ALT without statistical significance but significantly reduced levels of AST as compared with the control mice (Figures 1c and 2d). Mice from all the treatment groups had similar liver weights to those from the control group (Figure 1e). Mice in the control group receiving vehicle developed borderline MASH as indicated by a total MASH activity score (NAS) of 4.83 (Figure 1f). Notably, mice receiving continuous infusion of both low- and high-dose ALY688 showed significantly less ballooned hepatocytes and improved liver histology as indicated by ballooning and NAS and

a trend towards a lower degree of steatosis (Figure 1f). Subcutaneous injection of ALY688 at a high dose reduced NAS to a lesser extent than continuous infusion even at low dose, whereas injection of low-dose ALY688 slightly reduced the NAS without statistical significance (Figure 1f). These findings together demonstrate that ALY688 treatment is able to protect mice against the development of MASH. Sustained release of the peptide by osmotic pump is more effective than daily injection with the equivalent dose.

### A sustained release form of ALY688 attenuates the development of MASH

Since continuous release of ALY688 delivered by osmotic pump produced better effects than daily injection, we next evaluated the effect of a sustained release depot formulation designed for s.c. administration. First, we compared the pharmacokinetic profiles between the unmodified form (ALY688) and the sustained release form (ALY688-SR) by single s.c. injection of both forms of the peptide into male SD rats. A single injection of ALY688 resulted in a rapid and robust increase in the plasma concentration of ALY688 with a half-life of 0.45 h, whereas injection of ALY688-SR markedly extended the plasma half-life of ALY688 to 20.6 h (Figure S2). We then evaluated the effects of ALY688-SR on MASH in an improved mouse model that develops definite MASH.<sup>21</sup> In this model, mice were fed with CDAHf for a total period of 12 weeks to induce MASH. Treatment was started by s.c. injection of 3 or 15 mg kg<sup>-1</sup> day<sup>-1</sup> of ALY688-SR or vehicle at 3 weeks after initiation of CDAHf feeding, a timepoint when steatosis is established (Figure 2a). STC-fed mice treated with vehicle served as the negative control group without MASLD. Administration of ALY688-SR resulted in a significant increase in both serum and hepatic levels of ALY688 in a dose-dependent manner without affecting serum levels of adiponectin (Figure S3A–C). Treatment with either dose of ALY688-SR did not affect the body weight of mice fed with CDAHf (Figure 2b). High-dose ALY688-SR led to a mild, but significant, reduction of fat content and induction of lean content in mice (Figure S3D). Despite the lower body weight, mice fed with 12-week CDAHf exhibited liver injury as reflected by higher serum levels of ALT and AST as compared to the STC-fed mice (Figures 2c and 3d). They also showed increased liver weight and size with higher hepatic TG content (Figure 2e–g). Histological examination of liver sections by H&E staining demonstrated that there were extensive steatotic areas and inflammatory foci with a total NAS score of 5.25, indicative of MASH in CDAHf-fed mice (Figure 2c–g). Treatment with either low- or

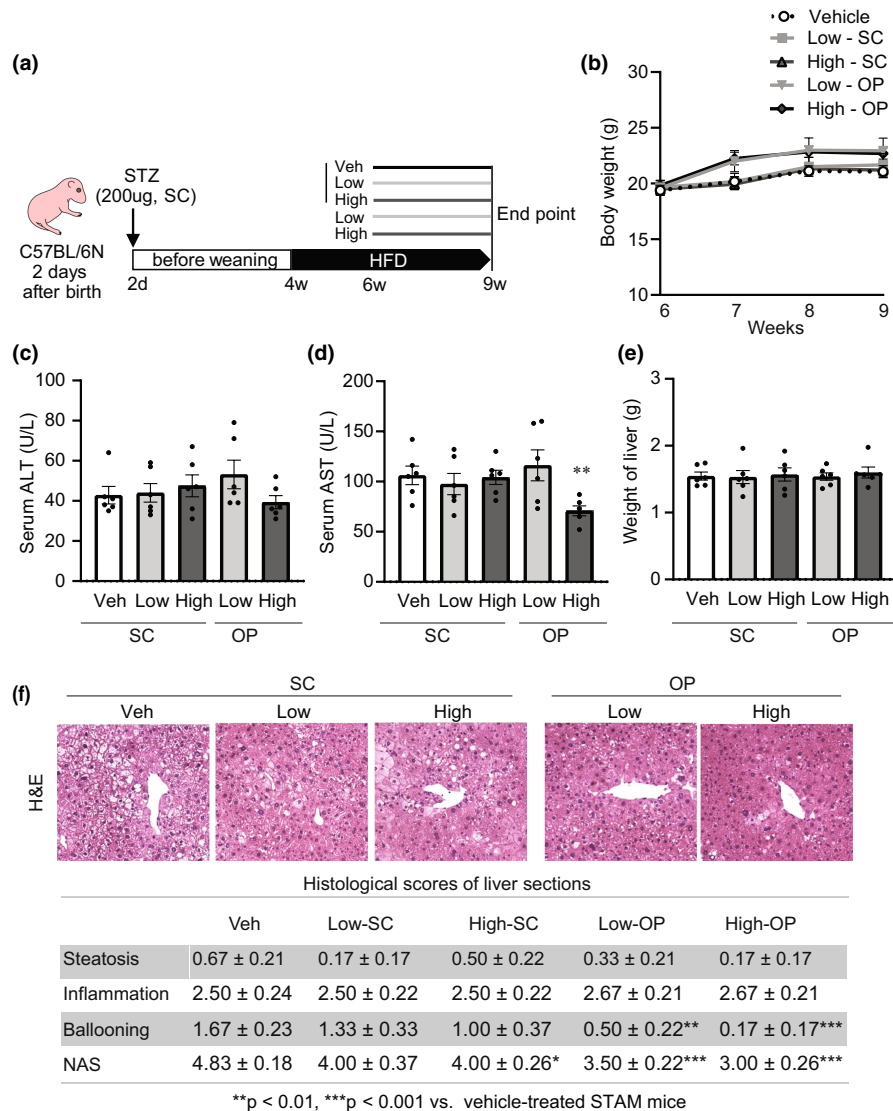


**FIGURE 1** ALY688 ameliorates the development of metabolic dysfunction-associated steatohepatitis (MASH) in streptozotocin and high-fat diet (STAM) mice. (a) Schematic diagram for induction of MASH in mice and the treatment regime. Male C57BL/6N mice at 2 days after birth received a single subcutaneous injection of 200 µg streptozotocin (STZ) solution; these mice were fed with a high-fat diet (HFD) from 4 to 9 weeks of age to induce MASH. From 6 to 9 weeks of age, the mice were administered with vehicle (veh) or two doses of ALY688 (low: 0.5 mg/kg/day, high: 5 mg/kg/day) via daily subcutaneous injection (SC) or continuous subcutaneous infusion via osmotic pumps (OP). (b) Body weight of the mice treated with vehicle or ALY688 during the treatment. Serum alanine transaminase (ALT) (c), serum aspartate transaminase (AST) (d), and liver weight (e) of the mice at the end of treatment. (f) Representative images of liver sections stained with hematoxylin and eosin (H&E) (scale bar, 100 µm). Lower panel, quantitative analyses of the grades of steatosis, inflammation, ballooning, and the total MASH activity score (NAS) for the H&E staining. Data represent mean ± standard error of the mean;  $n = 6$  per group; \* $p < 0.05$ , \*\* $p < 0.01$ , \*\*\* $p < 0.001$  versus veh-STC (standard chow), # $p < 0.05$ , ## $p < 0.01$ , ### $p < 0.001$  versus veh-CDAHFD (choline-deficient with low methionine high-fat diet).

high-dose ALY688-SR significantly reduced the serum ALT and AST levels (Figures 2c and 3d). Liver weight and hepatic TG content was significantly decreased in mice treated with high-dose ALY688-SR (Figures 2e and 3f). Histological examination revealed that low-dose ALY688-SR significantly reduced the degree of steatosis, whereas high-dose treatment decreased both steatosis and inflammation (Figure 2g). While treatment at a low dose led to a mild but significant decrease in the NAS

score by 10%, high-dose ALY688-SR led to a 23% reduction in the NAS score (Figure 2g). In contrast, administration of OCA, a farnesoid X receptor (FXR) agonist that was previously reported to protect against steatosis and fibrosis, <sup>29,30</sup> did not show beneficial effects on alleviating MASH even at a high dose (30 mg kg<sup>-1</sup> day<sup>-1</sup>, oral dosing) in our experimental model (Figure 2c–g). These findings strongly suggest that ALY688-SR is capable of effectively protecting against MASH development.



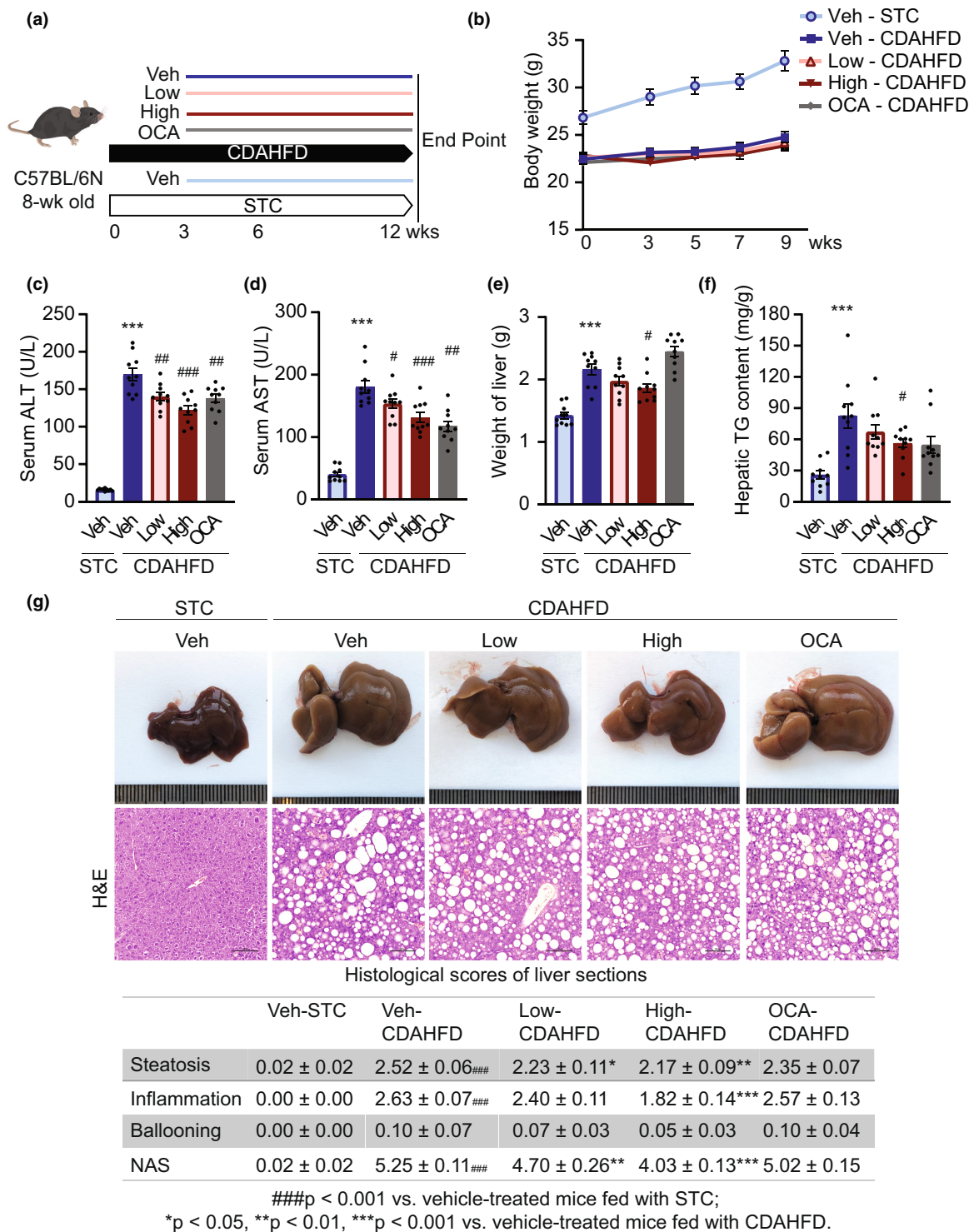


**FIGURE 2** Sustained release form of ALY688 (ALY688-SR) protects against diet-induced metabolic dysfunction-associated steatohepatitis (MASH) in mice. (a) Schematic diagram for establishment of diet-induced mouse model of MASH and the treatment regime. Male C57BL/6N mice at 8 weeks of age were fed with choline-deficient with low methionine high-fat diet (CDAHFD) for 12 weeks to induce MASH. Three weeks after CDAHFD feeding, the mice were treated with vehicle or ALY688-SR (low: 3 mg/kg/day, high: 15 mg/kg/day) by daily subcutaneous injection for 9 weeks. Obeticholic acid (OCA) was used as a positive control, standard chow (STC)-fed mice treated with vehicle were considered as the negative control group. (b) Body weight of the mice receiving vehicle (veh) or ALY688-SR during the treatment. Serum alanine transaminase (ALT) (c), aspartate transaminase (AST) (d), liver weight (e), and hepatic triglyceride (TG) concentration (f) of the mice at the end of treatment. Panel (g), representative gross photos of livers and histological images of liver sections stained with hematoxylin and eosin (H&E) (scale bar, 100  $\mu$ m). Lower panel, quantitative analyses of the grades of steatosis, inflammation, and the total MASH activity score for the H&E staining. Data represent mean  $\pm$  standard error of the mean;  $n = 10$  per group; \* $p < 0.05$ , \*\* $p < 0.01$ , \*\*\* $p < 0.001$  versus veh-STC, # $p < 0.05$ , ## $p < 0.01$ , ### $p < 0.001$  versus veh-CDAHFD (see also Figure S3).

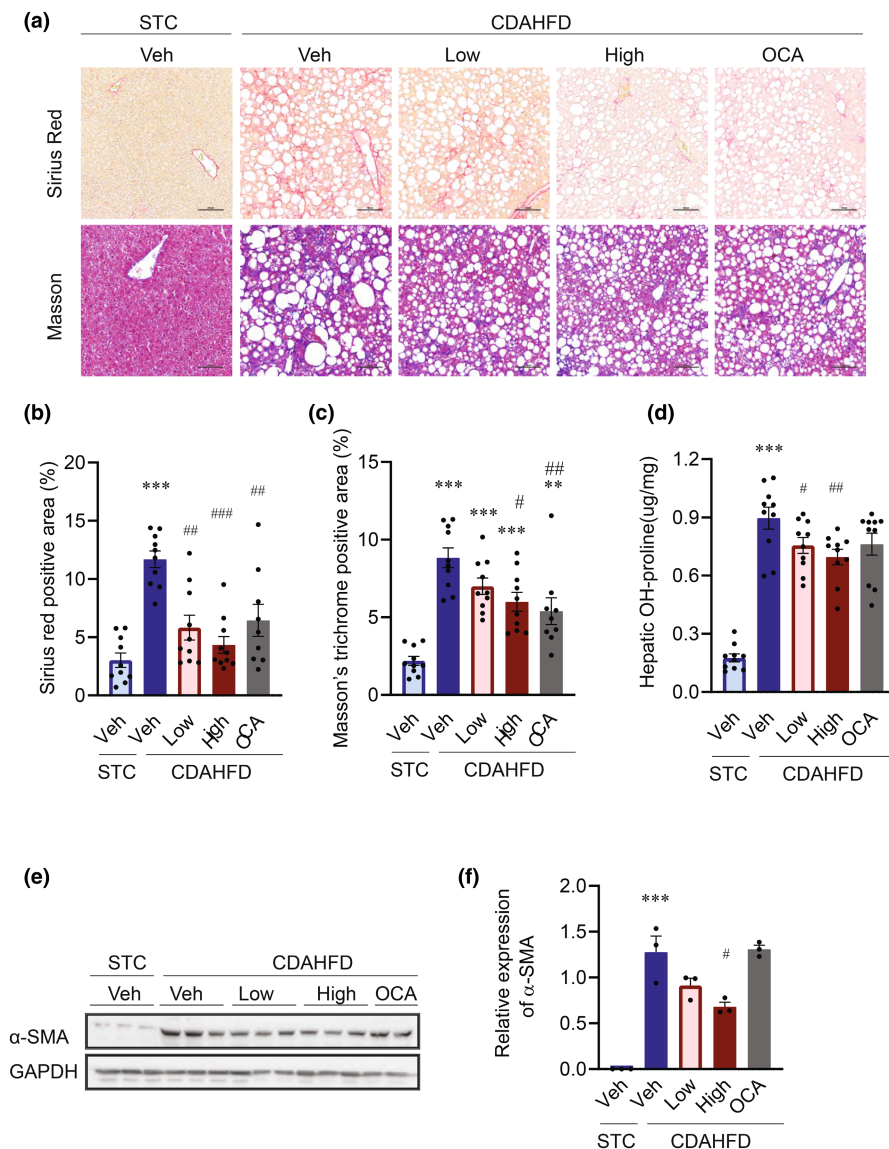


**FIGURE 3** ALY688-SR protects against metabolic dysfunction-associated steatohepatitis (MASH)-induced hepatic fibrosis in mice. (a) Representative images of liver sections from standard chow (STC) or choline-deficient with low methionine high-fat diet (CDAHFD)-fed mice treated with vehicle (veh) or ALY688-SR stained with Sirius red or Masson's trichrome (scale bar, 100  $\mu$ m). (b) Quantitative analysis for Sirius red staining. (c) Quantitative analysis for Masson's trichrome staining. (d) Hepatic hydroxyproline (OH-proline) content of the mice. (e) Western blot analysis for  $\alpha$ -SMA protein expression in the liver. The bottom panel is the densitometric analysis for the relative abundance of  $\alpha$ -SMA normalized with glyceraldehyde 3-phosphate dehydrogenase (GAPDH). (f) Quantitative analysis for  $\alpha$ -SMA. Data represent mean  $\pm$  standard error of the mean;  $n = 10$  per group; \* $p < 0.05$ , \*\* $p < 0.01$ , \*\*\* $p < 0.001$  versus veh-STC, # $p < 0.05$ , ## $p < 0.01$ , ### $p < 0.001$  versus veh-CDAHFD.

## ALY688-SR protects against MASH-related hepatic fibrosis

As sustained liver injury in MASH can lead to progressive fibrosis,<sup>31</sup> we further evaluated the severity of hepatic fibrosis in MASH mice treated with ALY688-SR. Histological analyses with both Sirius Red and Masson's trichrome staining demonstrated that the fibrotic area was significantly increased in the livers of mice fed with CDAHFD for 12 weeks (Figure 3a–c). Treatment with ALY688-SR markedly reduced the hepatic fibrotic area in mice with MASH, in a dose-dependent manner (Figure 3a–c). Consistent with the histological analyses, quantitative analysis of collagen by measuring hydroxyproline content in the liver supported the improvement of hepatic fibrosis by ALY688-SR treatment (Figure 3d). In addition, immunoblotting further confirmed down-regulation of hepatic expression of  $\alpha$ -SMA, a fibrotic marker, in mice treated with ALY688-SR (Figure 3e,f).

In line with previous reports, administration of OCA exhibited protective effects against hepatic fibrosis as demonstrated by histological examination (Figure 3a–c). However, ALY688-SR generally achieved greater effects in suppression of fibrosis at a 10-fold lower dose than OCA. These results collectively support a protective effect of ALY688-SR in halting the progression of MASH towards hepatic fibrosis.

## ALY688-SR up-regulates lipid catabolism, and down-regulates inflammation and fibrosis in the liver

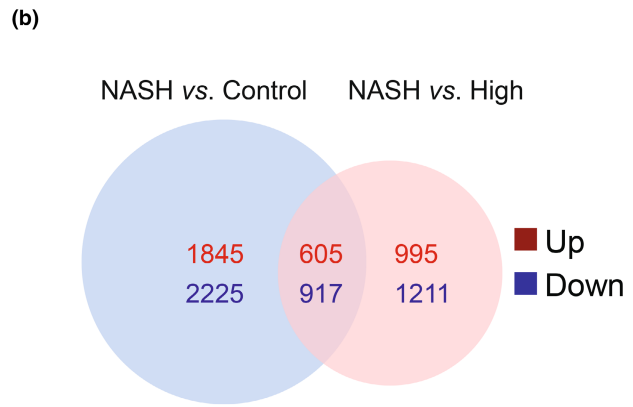
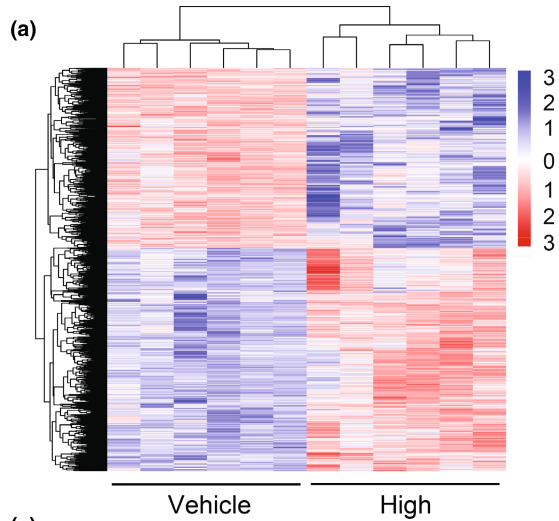
To gain mechanistic insights on the molecular basis underlying the effects of ALY688-SR in MASH, transcriptomic analysis of liver samples obtained from vehicle and high-dose ALY688-SR-treated mice fed with CDAHFD was performed. Among 27,467 transcripts assessed by

RNA sequencing (RNA-seq), there were 1600 genes significantly down-regulated and 2128 genes significantly up-regulated following ALY688-SR treatment (false discovery rate [FDR] adjusted  $p \leq 0.05$ ; Figure 4a). To further identify the differentially expressed genes (DEGs) induced by ALY688 treatment that may be involved in the development of MASH, we incorporated our dataset into the publicly available RNA-seq dataset: hepatic gene expression profiles in MASH mice fed with a high-fat, cholesterol, and fructose diet for 24 weeks versus healthy mice fed a chow diet.<sup>32</sup> Among the DEGs between the MASH and the healthy liver, ALY688-SR treatment significantly reversed 605 of 2450 up-regulated genes and 917 of 3142 down-regulated genes mediated by MASH (Figure 4b). Unbiased gene ontology (GO) enrichment analysis revealed that the genes decreased in MASH and induced by ALY688-SR treatment were enriched for lipid catabolism, whereas the genes increased in MASH and suppressed by ALY688-SR treatment were enriched for inflammatory response and fibrosis (Figure 4c,d). We also examined expression patterns of key genes involved in fatty acid oxidation (*Acot1*, *Acox1*, *Cyp4a12*), fibrosis (*Tgfb*, *Col1a1*, *Timp1*), and inflammation (*Tnfa*, *Mcp1*, *IL-1 $\beta$* ) in the liver of mice from all the experimental groups. Hepatic expression levels of genes involved in fatty acid oxidation were significantly down-regulated in CDAHf-fed mice as compared to STC-fed mice, but they were restored by treatment with ALY688-SR, especially at the high concentration, and OCA (Figure 4e). By contrast, the expression levels of key genes related to inflammation were markedly induced in the liver of CDAHf-fed mice (Figure 4g). However, the induction of these genes was significantly reduced by high-dose ALY688-SR treatment (Figure 4g). Notably, OCA treatment failed to reverse the expression of MASH-induced inflammatory genes (Figure 4g). Similarly, fibrosis-related genes were induced in the MASH liver, but both low- and high-dose ALY688-SR treatment effectively suppressed these genes relative to the vehicle treatment (Figure 4f). Treatment with OCA appeared to reduce the expression of most of these fibrotic genes, although without statistical significance (Figure 4f). Furthermore, based on the regulatory network, the control over lipid catabolism in ALY688-SR-treated mice appeared to be predominantly regulated by transcription factors HNF1 $\alpha$ , NR3C2, ETV1, PPAR $\alpha$ , HNF4 $\alpha$ , and ARNT, whereas the transcriptional control over inflammation and fibrosis appeared to be mainly regulated by JUN, TRP53, NFKB1, NFE2L2, AHR, SMAD1, FOSL1, SP1, JUN, and NFIC (Figure 4h,i). Taken together, these findings suggest that ALY688-SR effectively reversed MASH-induced genes and pathways back to the normal levels, especially in relation to lipid catabolism, inflammation, and fibrosis.

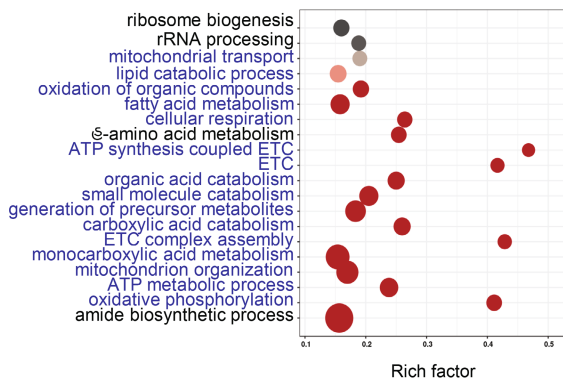
## DISCUSSION AND CONCLUSIONS

Although adiponectin has been demonstrated to have protective effects against MASH, therapeutic development of native adiponectin protein has been restricted by a number of challenges, including short plasma half-life and poor druggable properties (i.e., insolubility and multimeric isoforms). ALY688 is an adiponectin-based short peptide with good stability in mouse plasma, excellent safety profile, and protective effects against CCL<sub>4</sub> and TAA-induced liver injuries.<sup>18,19</sup> In the present study we investigated the efficacy of ALY688 on MASH in mouse models. We found that intervention with the unmodified form of ALY688 by continuous infusion reduced disease severity in the STAM model to a larger extent than that with daily s.c. injection, suggesting that sustained release of the peptide is more effective than daily injection with the equivalent dose. We further tested the effects of a sustained release form, ALY688-SR, on MASH in a CDAHf-induced mouse model, and found that it markedly alleviated MASH and its related fibrosis. The improved efficacy of ALY688-SR against MASH and fibrosis is presumed to be attributed to its greatly extended plasma half-life of 20.6 h compared to 0.45 h for the unmodified form, according to our pharmacokinetic study performed with rats. Mechanistically, ALY688-SR alleviated the disease by increasing lipid catabolism and eliminating inflammation and fibrosis in the liver.

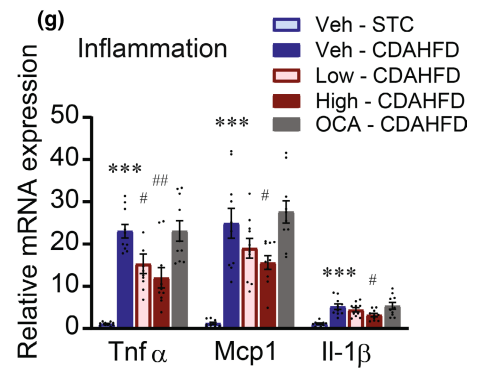
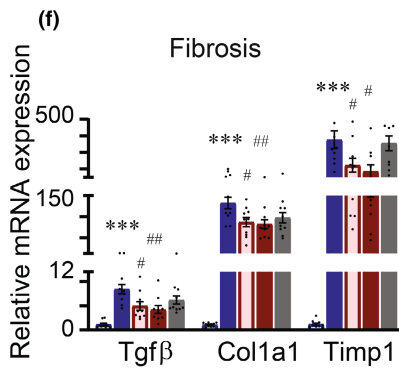
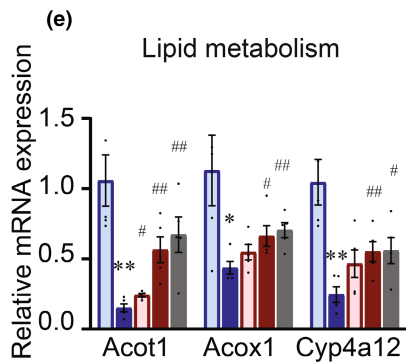
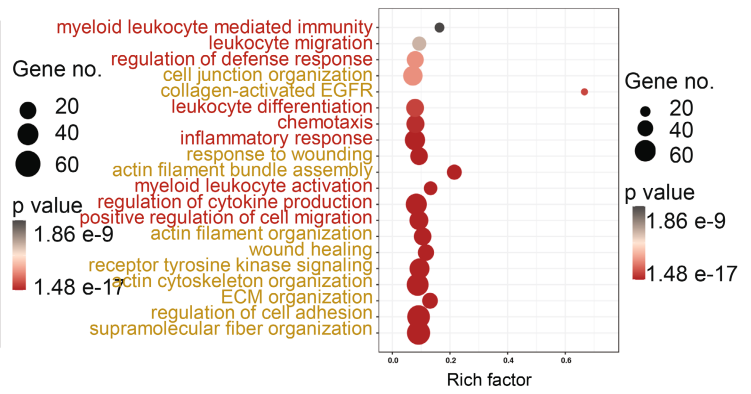
The role of adiponectin in the regulation of lipid metabolism in the liver has been well documented in previous studies. Treatment of primary rat hepatocytes with adiponectin in vitro markedly increased insulin sensitivity.<sup>34</sup> Infusion of full-length recombinant adiponectin suppressed de novo lipogenesis and induced fatty acid oxidation in the liver of *ob/ob* mice with steatosis.<sup>15</sup> In addition to these direct effects on the liver, adiponectin also strongly induced fatty acid oxidation in skeletal muscles,<sup>35</sup> thereby limiting the influx of circulating fatty acid into the liver. In line with these findings, we have demonstrated that administration of ALY688-SR reduced hepatic lipid accumulation and the steatosis score in CDAHf-fed mice (Figure 2f,g). Additionally, transcriptomic analysis of liver revealed that treatment with ALY688-SR induced hepatic expression of genes involved in fatty acid oxidation that were suppressed in MASH (Figure 4c,e). Our in vitro experiments with human induced pluripotent stem (iPS) cell-derived hepatocytes demonstrated that ALY688 activated AMPK (SF 1D), the canonical adiponectin-mediated signaling pathway that is involved in the activation PPAR $\alpha$ .<sup>36</sup> Since PPAR $\alpha$  is a key transcription factor controlling the expression of a number of genes involved in peroxisomal and mitochondrial  $\beta$ -oxidation,<sup>36</sup> it is likely that ALY688



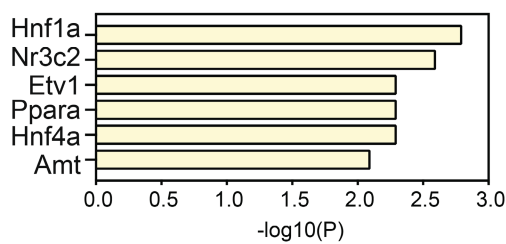
(c) Downregulated by NASH, upregulated by ALY688



(d) Upregulated by NASH, downregulated by ALY688



(h) TFs for DEGs downregulated by NASH, upregulated by ALY688



(i) TFs for DEGs upregulated by NASH, downregulated by ALY688

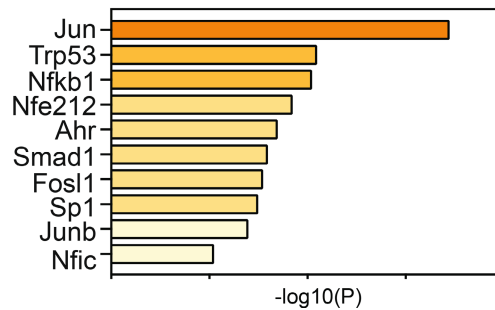


**FIGURE 4** ALY688-SR improves lipid metabolism, reduces inflammation and fibrosis in the liver in mice with metabolic dysfunction-associated steatohepatitis (MASH). (a–d) After 9 weeks of treatment, liver samples from vehicle (veh) and high-dose ALY688-SR-treated mice fed with choline-deficient with low methionine high-fat diet (CDAHFD) were harvested for transcriptomic analysis. (a) Heat map illustrates all differentially expressed transcripts (adjusted  $p$ -value  $< 0.05$ ) in the liver. Colors refer to gene expression  $z$ -score. (b) Venn diagram identifies the genes induced by MASH and reversed by ALY688-SR treatment or suppressed by MASH and reversed by ALY688-SR treatment. The publicly available dataset (MASH vs. Control: GSE162249) was used for the analysis. Gene ontology (GO) enrichment analysis of the genes downregulated by MASH and upregulated by ALY688-SR (c) and upregulated by MASH and downregulated by ALY688-SR (d). The top 20 regulated pathways are shown.  $n = 6$  per group. Real-time polymerase chain reaction was performed to determine the mRNA expression of genes related to lipid metabolism (e), fibrosis (f), and inflammation (g) in the livers of the indicated groups. Data represent mean  $\pm$  standard error of the mean;  $n = 10$  per group; \* $p < 0.05$ , \*\* $p < 0.01$ , \*\*\* $p < 0.001$  versus veh-STC, # $p < 0.05$ , ## $p < 0.01$ , ### $p < 0.001$  versus veh-CDAHFD. (h, i) TRRUST database<sup>33</sup> was used to create a transcriptional regulatory model using the 917 differentially expressed genes (DEGs) downregulated by MASH, upregulated by ALY688-SR (h) and the 605 DEGs upregulated by MASH, downregulated by ALY688-SR (adjusted  $p < 0.01$ ).

may attenuate hepatic steatosis by induction of fatty acid  $\beta$ -oxidation through a AMPK-PPAR $\alpha$ -dependent pathway. Indeed, PPAR $\alpha$  was identified as an upstream regulator of DEGs after ALY688 treatment by in silico prediction (Figure 4h). In addition, HNF1 $\alpha$  and HNF4 $\alpha$ , master regulators of lipid metabolism in the liver, were also predicted to control ALY688-mediated genes. This is partially in line with a previous study showing that interaction of HNF4 $\alpha$  with promoter regions of genes encoding several key metabolic enzymes in the liver was reduced in adiponectin knockout mice.<sup>37</sup>

Hepatic inflammation fuels the transition from steatosis to MASH and is an important driving force of fibrogenesis.<sup>38</sup> Targeting inflammation has been shown to be a promising approach for treatment of MASH. In particular, CC motif chemokine receptor (CCR) 2/5 antagonist and apoptosis signaling kinase-1 (ASK1) inhibitor targeting inflammatory response has been shown to resolve MASH and fibrosis in early clinical trials.<sup>39</sup> However, since these approaches failed in phase III trials, there is an urgent need to discover additional anti-inflammatory candidates for potential therapy. The anti-inflammatory properties of adiponectin have been well studied. Adiponectin suppresses the secretion of lipopolysaccharide (LPS)-stimulated TNF $\alpha$  production and induces the secretion of anti-inflammatory cytokine IL-10 in cultured human macrophages.<sup>40</sup> Adiponectin is required for polarization of macrophages to an anti-inflammatory M2 phenotype both in vitro and in vivo.<sup>41</sup>

In the present study, we found that the overall histological improvement in the livers of mice receiving ALY688 treatment was predominantly driven by reduced lobular inflammation (Figure 2g), confirming the anti-inflammatory effects of ALY688. Our RNA-seq analysis further demonstrated that pathways enriched for leukocyte migration and cytokine production were upregulated in MASH and suppressed by ALY688 intervention (Figure 4d). Additionally, administration of ALY688 significantly reduced hepatic expression of pro-inflammatory cytokines, as shown by RT-PCR analysis (Figure 4g). In

silico analysis predicted c-Jun and NF $\kappa$ B as the top transcription factors regulating genes induced in MASH but suppressed by ALY688 treatment (Figure 4i). In line with these results, it was reported by previous studies that activation of NF $\kappa$ B and JNK (the latter is the c-Jun activator) contributes to hepatic inflammation and the pathogenesis of MASH.<sup>42</sup> Moreover, pretreatment of human macrophages with adiponectin inhibits phosphorylation of NF $\kappa$ B and JNK.<sup>43</sup> Overall, these findings collectively suggest that ALY688-SR intervention alleviates hepatic inflammation associated with MASH severity, possibly through the NF $\kappa$ B and JNK signaling pathways.

Fibrosis is an important indicator of disease progression of MASH. The extent of liver fibrosis is the major risk for cardiovascular comorbidity and mortality in MASH.<sup>44</sup> During development of MASH, hepatocyte death and inflammation predispose hepatic stellate cells (HSCs) to transdifferentiate from a quiescent, vitamin A storing state, to activated,  $\alpha$ -SMA-positive myofibroblasts. These myofibroblasts are the major source of extracellular matrix that leads to liver fibrosis.<sup>45</sup> Most genetic and dietary models of MASH do not exhibit prominent hepatic fibrosis within a short period of time, typically within 4–5 months.<sup>46</sup> In our study, mice fed with CDAHFD developed MASH with fibrosis within 12 weeks (Figure 4). Liver fibrosis was markedly reduced by ALY688 treatment (Figure 3a–c). Furthermore, MASH-mediated induction of hepatic  $\alpha$ -SMA expression was also significantly reduced by ALY688-SR (Figure 3d), indicating that HSC activation during MASH was suppressed by ALY688-SR. TGF $\beta$  is the most potent inducer of hepatic fibrosis, as it activates HSCs and inhibits the apoptosis of activated HSCs.<sup>47</sup> Serum level of TGF $\beta$  is positively correlated with the severity of fibrosis in patients with MASLD.<sup>48</sup> The present study showed that hepatic expression levels of TGF $\beta$  were induced in mice fed with 12-week CDAHFD, but significantly attenuated by ALY688-SR treatment (Figure 3f). TGF $\beta$  exerts its effects mainly via small mothers against decapentaplegic (SMAD)-dependent pathways.<sup>49</sup> SMAD1 was identified as an upstream regulator of the genes induced in mice with

MASH and reduced by ALY688-SR intervention according to in silico analysis (Figure 3i), suggesting the protective effect of ALY688-SR against fibrosis is likely through inhibition of the TGF $\beta$ -SMAD1 signaling.

OCA is a synthetic bile acid with highly selective agonistic activity on FXR, a nuclear receptor that regulates the metabolism of bile acids, lipids, and glucose.<sup>50</sup> Previous animal studies showed that OCA improved hepatic steatosis and inflammation in various murine models of MASH,<sup>51</sup> therefore OCA was used as a positive control for MASH treatment in our study. However, we found that OCA did not exhibit a significant effect on hepatic steatosis or inflammation according to the gold standard criteria of liver histology (Figure 2g). Instead, hepatic fibrosis was significantly curtailed in mice treated with OCA, which contributed to the lower level of liver injury in these mice (Figure 3). Although OCA was demonstrated to mainly protect against steatosis and inflammation in previous preclinical studies, it did not show statistically significant resolution of MASH but reduced liver fibrosis in the phase III clinical trial (NCT02548351). The discrepancy between the results from previous preclinical studies and ours can be reconciled by considering the use of different murine models of MASH, which exhibit varying histopathological and metabolic features and demonstrate different drug responsiveness.<sup>46</sup>

Although we have provided in vivo evidence demonstrating the anti-steatotic, anti-inflammatory, and anti-fibrotic effects of ALY688-SR in a mouse model of MASH, the direct molecular targets and signaling pathways conferring these effects of ALY688-SR remain undetermined. Furthermore, the conclusions drawn from this study were based on two mouse models of MASH, including a STAM model and a CDAHf-fed mouse model, which do not exhibit weight loss during MASH development compared to the MCD model. However, there is a possibility that they may not fully recapitulate the features of MASH observed in humans, which are typically associated with metabolic dysfunctions. The effectiveness of ALY688-SR for MASH therapy in patients remains to be determined in future clinical studies. Notably, the STAM mouse model was not fully progressed to MASH, but developed borderline MASH instead, therefore ALY688-SR effectively reversed MASLD. Additionally, in the CDAHf-induced mouse model of definite MASH, since the mice were treated with ALY688-SR at the timepoint when steatosis, but not MASH, is developed, the present study only demonstrated the protective effects of ALY688-SR on MASH. Further studies are required to evaluate its effects on reversal of MASH and its related hepatic fibrosis.

Overall, our study showed that the adiponectin analogue ALY688-SR exerted multiple beneficial effects in the liver, including inhibition of steatosis, inflammation, and fibrosis, thus protecting against the development and

progression of MASH in both induced MASH models. These actions are likely to be attributed to the activation of adiponectin-mediated signaling, such as AMPK. Sustained release formulation of the peptide produced better effects in alleviating MASH and its related fibrosis, supporting its potential therapeutic application for the diseases in clinic.

#### AUTHOR CONTRIBUTIONS

Z.H., X.Y., and H.K.S. wrote the manuscript. Z.H., A.X., and G.S. designed the research. Z.H., S.H., L.J., Q.W., X.W., and H.K.S. performed the research and analyzed the data. H.H.H., A.P., and K.C. contributed new reagents.

#### ACKNOWLEDGMENTS

We would like to acknowledge the contribution of Dr. Kristin Schram in generating Figure 5.

#### FUNDING INFORMATION


This study was supported by Allysta Pharmaceuticals Inc., and in part by the Area of Excellence (AOE/M/707-18) from the Research Grant Council of Hong Kong and the Health and Medical Research Fund.

#### CONFLICT OF INTEREST STATEMENT

H.H.H. is the Chief Executive Officer of Allysta Pharmaceuticals Inc. (Bellevue, WA, USA), a pharmaceutical company developing ALY688 against various diseases. A.P. and K.C. are Principal Scientist and Head of Preclinical Development of Allysta Pharmaceuticals Inc., respectively. G.S. consults for Allysta Pharmaceuticals Inc. All other authors declared no competing interests for this work.

#### ORCID

Zhe Huang  <https://orcid.org/0000-0003-4943-3723>

Hye Kyoung Sung  <https://orcid.org/0000-0002-4674-3796>

Xingqun Yan  <https://orcid.org/0000-0002-5909-1205>

Shiyu He  <https://orcid.org/0009-0006-9397-3865>

Leigang Jin  <https://orcid.org/0000-0002-6916-4009>

Qin Wang  <https://orcid.org/0000-0002-6138-359X>

Xuerui Wu  <https://orcid.org/0000-0002-5917-3278>

Henry H. Hsu  <https://orcid.org/0009-0002-8018-2651>

Angelica Pignalosa  <https://orcid.org/0000-0002-7136-5950>

Kathryn Crawford  <https://orcid.org/0009-0008-7037-2383>

Gary Sweeney  <https://orcid.org/0000-0002-1946-1347>

Aimin Xu  <https://orcid.org/0000-0002-0668-033X>

Aimin Xu  <https://orcid.org/0000-0002-0668-033X>

#### REFERENCES

- Chan WK, Chuah KH, Rajaram RB, Lim LL, Ratnasingam J, Vethakkan SR. Metabolic dysfunction-associated steatotic liver

- disease (MASLD): a state-of-the-art review. *J Obes Metab Syndr*. 2023;32(3):197-213.
2. Diehl AM, Day C. Cause, pathogenesis, and treatment of nonalcoholic steatohepatitis. *N Engl J Med*. 2017;377(21):2063-2072.
  3. Garuti F, Neri A, Avanzato F, et al., the ITA.LI.CA study group. The changing scenario of hepatocellular carcinoma in Italy: an update. *Liver Int* 2021;41(3):585-597.
  4. Sacco R, Ramai D, Tortora R, et al., A.I.G.O. (Italian Association of Hospital Gastroenterologists). Role of etiology in hepatocellular carcinoma patients treated with lenvatinib: a counterfactual event-based mediation analysis. *Cancers (Basel)* 2023;15(2):381-392.
  5. Machado MV, Diehl AM. Pathogenesis of nonalcoholic steatohepatitis. *Gastroenterology*. 2016;150(8):1769-1777.
  6. Scherer PE, Williams S, Fogliano M, Baldini G, Lodish HF. A novel serum protein similar to C1q, produced exclusively in adipocytes. *J Biol Chem* 1995;270(45):26746-26749.
  7. Yamauchi T, Kamon J, Ito Y, et al. Cloning of adiponectin receptors that mediate antidiabetic metabolic effects. *Nature* 2003;423(6941):762-769.
  8. Arita Y, Kihara S, Ouchi N, et al. Paradoxical decrease of an adipose-specific protein, adiponectin, in obesity. *Biochem Biophys Res Commun*. 1999;257(1):79-83.
  9. Hui JM, Hodge A, Farrell GC, Kench JG, Kriketos A, George J. Beyond insulin resistance in NASH: TNF-alpha or adiponectin? *Hepatology*. 2004;40(1):46-54.
  10. Pajvani UB, Hawkins M, Combs TP, et al. Complex distribution, not absolute amount of adiponectin, correlates with thiazolidinedione-mediated improvement in insulin sensitivity. *J Biol Chem*. 2004;279(13):12152-12162.
  11. Bianchi G, Bugianesi E, Frystyk J, Tarnow L, Flyvbjerg A, Marchesini G. Adiponectin isoforms, insulin resistance and liver histology in nonalcoholic fatty liver disease. *Dig Liver Dis*. 2011;43(1):73-77.
  12. Kamada Y, Matsumoto H, Tamura S, et al. Hypoadiponectinemia accelerates hepatic tumor formation in a nonalcoholic steatohepatitis mouse model. *J Hepatol*. 2007;47(4):556-564.
  13. Fukushima J, Kamada Y, Matsumoto H, et al. Adiponectin prevents progression of steatohepatitis in mice by regulating oxidative stress and Kupffer cell phenotype polarization. *Hepatol Res*. 2009;39(7):724-738.
  14. Nakayama H, Otabe S, Yuan X, et al. Effects of adiponectin transgenic expression in liver of nonalcoholic steatohepatitis model mice. *Metabolism*. 2009;58(7):901-908.
  15. Xu A, Wang Y, Keshaw H, Xu LY, Lam KS, Cooper GJ. The fat-derived hormone adiponectin alleviates alcoholic and nonalcoholic fatty liver diseases in mice. *J Clin Invest*. 2003;112(1):91-100.
  16. Heiker JT, Klotting N, Bluher M, Beck-Sickinger AG. Access to gram scale amounts of functional globular adiponectin from *E. coli* inclusion bodies by alkaline-shock solubilization. *Biochem Biophys Res Commun*. 2010;398(1):32-37.
  17. Fisher FM, Trujillo ME, Hanif W, et al. Serum high molecular weight complex of adiponectin correlates better with glucose tolerance than total serum adiponectin in Indo-Asian males. *Diabetologia*. 2005;48(6):1084-1087.
  18. Otvos L Jr, Haspinger E, La Russa F, et al. Design and development of a peptide-based adiponectin receptor agonist for cancer treatment. *BMC Biotechnol*. 2011;11:90.
  19. Wang H, Zhang H, Zhang Z, et al. Adiponectin-derived active peptide ADP355 exerts anti-inflammatory and anti-fibrotic activities in thioacetamide-induced liver injury. *Sci Rep*. 2016;6:19445.
  20. Xu H, Zhao Q, Song N, et al. AdipoR1/AdipoR2 dual agonist recovers nonalcoholic steatohepatitis and related fibrosis via endoplasmic reticulum-mitochondria axis. *Nat Commun*. 2020;11(1):5807.
  21. Matsumoto M, Hada N, Sakamaki Y, et al. An improved mouse model that rapidly develops fibrosis in non-alcoholic steatohepatitis. *Int J Exp Pathol*. 2013;94(2):93-103.
  22. Fujii M, Shibazaki Y, Wakamatsu K, Honda Y, Kawauchi Y, Suzuki K, Arumugam S, Watanabe K, Ichida T, Asakura H, Yoneyama H. A murine model for non-alcoholic steatohepatitis showing evidence of association between diabetes and hepatocellular carcinoma. *Med Mol Morphol* 2013;46(3):141-152.
  23. Ye D, Wang Y, Li H, et al. Fibroblast growth factor 21 protects against acetaminophen-induced hepatotoxicity by potentiating peroxisome proliferator-activated receptor coactivator protein-1alpha-mediated antioxidant capacity in mice. *Hepatology*. 2014;60(3):977-989.
  24. Yin Z, Murphy MC, Li J, et al. Prediction of nonalcoholic fatty liver disease (NAFLD) activity score (NAS) with multiparametric hepatic magnetic resonance imaging and elastography. *Eur Radiol*. 2019;29(11):5823-5831.
  25. Liang W, Menke AL, Driessen A, et al. Establishment of a general NAFLD scoring system for rodent models and comparison to human liver pathology. *PLoS One*. 2014;9(12):e115922.
  26. Zhang X, Shen J, Man K, et al. CXCL10 plays a key role as an inflammatory mediator and a non-invasive biomarker of non-alcoholic steatohepatitis. *J Hepatol*. 2014;61(6):1365-1375.
  27. Ye D, Yang K, Zang S, et al. Lipocalin-2 mediates non-alcoholic steatohepatitis by promoting neutrophil-macrophage crosstalk via the induction of CXCR2. *J Hepatol*. 2016;65(5):988-997.
  28. Wu X, Motoshima H, Mahadev K, Stalker TJ, Scalia R, Goldstein BJ. Involvement of AMP-activated protein kinase in glucose uptake stimulated by the globular domain of adiponectin in primary rat adipocytes. *Diabetes* 2003;52(6):1355-1363.
  29. Verbeke L, Mannaerts I, Schierwagen R, et al. FXR agonist obeticholic acid reduces hepatic inflammation and fibrosis in a rat model of toxic cirrhosis. *Sci Rep*. 2016;6:33453.
  30. Goto T, Itoh M, Suganami T, et al. Obeticholic acid protects against hepatocyte death and liver fibrosis in a murine model of nonalcoholic steatohepatitis. *Sci Rep*. 2018;8(1):8157.
  31. Friedman SL. Liver fibrosis in 2012: convergent pathways that cause hepatic fibrosis in NASH. *Nat Rev Gastroenterol Hepatol*. 2013;10(2):71-72.
  32. Lee SM, Pusec CM, Norris GH, et al. Hepatocyte-specific loss of PPARgamma protects mice from NASH and increases the therapeutic effects of rosiglitazone in the liver. *Cell Mol Gastroenterol Hepatol*. 2021;11(5):1291-1311.
  33. Han H, Cho J, Lee S, et al. TRRUST v2: an expanded reference database of human and mouse transcriptional regulatory interactions. *Nucleic Acids Res*. 2018;46(D1):D380-D386.
  34. Wang Y, Xu A, Knight C, Xu LY, Cooper GJ. Hydroxylation and glycosylation of the four conserved lysine residues in the collagenous domain of adiponectin. Potential role in the modulation of its insulin-sensitizing activity. *J Biol Chem*. 2002;277(22):19521-19529.

35. Yamauchi T, Kamon J, Minokoshi Y, et al. Adiponectin stimulates glucose utilization and fatty-acid oxidation by activating AMP-activated protein kinase. *Nat Med*. 2002;8(11):1288-1295.
36. Yoon MJ, Lee GY, Chung JJ, Ahn YH, Hong SH, Kim JB. Adiponectin increases fatty acid oxidation in skeletal muscle cells by sequential activation of AMP-activated protein kinase, p38 mitogen-activated protein kinase, and peroxisome proliferator-activated receptor alpha. *Diabetes*. 2006;55(9):2562-2570.
37. Liu Q, Yuan B, Lo KA, Patterson HC, Sun Y, Lodish HF. Adiponectin regulates expression of hepatic genes critical for glucose and lipid metabolism. *Proc Natl Acad Sci U S A*. 2012;109(36):14568-14573.
38. Schuster S, Cabrera D, Arrese M, Feldstein AE. Triggering and resolution of inflammation in NASH. *Nat Rev Gastroenterol Hepatol*. 2018;15(6):349-364.
39. Vuppalanchi R, Noureddin M, Alkhoufi N, Sanyal AJ. Therapeutic pipeline in nonalcoholic steatohepatitis. *Nat Rev Gastroenterol Hepatol* 2021;18(6):373–392.
40. Kumada M, Kihara S, Ouchi N, et al. Adiponectin specifically increased tissue inhibitor of metalloproteinase-1 through interleukin-10 expression in human macrophages. *Circulation*. 2004;109(17):2046-2049.
41. Hui X, Gu P, Zhang J, et al. Adiponectin enhances cold-induced browning of subcutaneous adipose tissue via promoting M2 macrophage proliferation. *Cell Metab*. 2015;22(2):279-290.
42. Dorn C, Engelmann JC, Saugspier M, et al. Increased expression of c-Jun in nonalcoholic fatty liver disease. *Lab Invest*. 2014;94(4):394-408.
43. Folco EJ, Rocha VZ, Lopez-Ilasaca M, Libby P. Adiponectin inhibits pro-inflammatory signaling in human macrophages independent of interleukin-10. *J Biol Chem*. 2009;284(38):25569-25575.
44. Angulo P, Kleiner DE, Dam-Larsen S, et al. Liver fibrosis, but no other histologic features, is associated with long-term outcomes of patients with nonalcoholic fatty liver disease. *Gastroenterology*. 2015;149(2):389-397 e10.
45. Bataller R, Brenner DA. Liver fibrosis. *J Clin Invest*. 2005;115(2):209-218.
46. Farrell G, Schattenberg JM, Leclercq I, et al. Mouse models of nonalcoholic steatohepatitis: toward optimization of their relevance to human nonalcoholic steatohepatitis. *Hepatology*. 2019;69(5):2241-2257.
47. Dewidar B, Meyer C, Dooley S, Meindl-Beinker AN. TGF- $\beta$  in hepatic stellate cell activation and liver fibrogenesis-updated 2019. *Cells* 2019;8(11):1419-1453.
48. Mahmoud AA, Bakir AS, Shabana SS. Serum TGF- $\beta$ , serum MMP-1, and HOMA-IR as non-invasive predictors of fibrosis in Egyptian patients with NAFLD. *Saudi J Gastroenterol*. 2012;18(5):327-333.
49. Walton KL, Johnson KE, Harrison CA. Targeting TGF- $\beta$  mediated SMAD signaling for the prevention of fibrosis. *Front Pharmacol*. 2017;8:461.
50. Wang YD, Chen WD, Moore DD, Huang W. FXR: a metabolic regulator and cell protector. *Cell Res*. 2008;18(11):1087-1095.
51. Yang ZY, Liu F, Liu PH, et al. Obeticholic acid improves hepatic steatosis and inflammation by inhibiting NLRP3 inflammasome activation. *Int J Clin Exp Pathol*. 2017;10(8):8119-8129.

## SUPPORTING INFORMATION

Additional supporting information can be found online in the Supporting Information section at the end of this article.

**How to cite this article:** Huang Z, Sung HK, Yan X, et al. The adiponectin-derived peptide ALY688 protects against the development of metabolic dysfunction-associated steatohepatitis. *Clin Transl Sci*. 2024;17:e13760. doi:[10.1111/cts.13760](https://doi.org/10.1111/cts.13760)